Hindawi
International Journal of Geophysics
Volume 2018, Article ID 4931307, 19 pages
https://doi.org/10.1155/2018/4931307

Research Article

3D Seismic Structural Analysis and Basin Modeling of the Matruh Basin, Western Desert, Egypt

Farouk I. Metwalli,[1] **El Arabi H. Shendi**,[2] **Bruce Hart**,[3] **and Waleed M. Osman**[4]

[1]*Geology Department, Faculty of Science, Helwan University, Cairo, Egypt*
[2]*Geology Department, Faculty of Science, Suez Canal University, Ismailia, Egypt*
[3]*Earth and Planetary Science Department, Faculty of Science, McGill University, Montréal, QC, Canada*
[4]*Department of Science and Mathematics, Faculty of Mining and Petroleum Engineering, Suez Canal University, Suez, Egypt*

Correspondence should be addressed to Farouk I. Metwalli; pine_egypt@hotmail.com

Received 30 August 2017; Accepted 29 November 2017; Published 18 January 2018

Academic Editor: Rudolf A. Treumann

In order to evaluate the hydrocarbon potential of the Matruh Basin, North Western Desert of Egypt, the tectonic history, basin analysis, and maturity modeling of the Albian-Cenomanian Formations of the Matruh Basin were investigated using well logs and 3D seismic data. Structural analysis of the tops of the Bahariya, Kharita, and Alamein Dolomite Formations reveals them to dip to the southeast. Burial history and subsidence curves show that the basin experienced a tectonic subsidence through the Middle-Late Jurassic and Early Cretaceous times. Thermal maturity models indicated that Cenomanian clastics of the Bahariya Formation are in the early mature stage in the east portions of the area, increasing to the mid maturity level in the southwestern parts. On the other hand, the Albian Kharita Formation exhibits a mid maturation level in the most parts of the area. The petroleum system of the Matruh Basin includes a generative (charge) subsystem with Middle Jurassic and Cenomanian sources (for oil/gas) and Turonian sources (for oil), with peak generation from Turonian to Eocene, and a migration-entrapment subsystem including expulsion and migration during Early Tertiary to Miocene into structures formed from Late Cretaceous to Eocene.

1. Introduction

The area of investigation is located in the northwestern part of the Western Desert of Egypt, in the northern part of the Western Desert Basin (Figure 1). The Western Desert covers more than two-thirds of the area of Egypt. Within Egypt Dolson et al. [1] showed that whereas the Gulf of Suez has reached a mature discovery rate, both the offshore Mediterranean and the Western Desert areas hold significant promise. They suggested that some reservoirs of 100 MMBO and larger would be discovered in the Western Desert. Indeed, several significant discoveries in this area in the past few years suggest that this area of Egypt and adjacent Libya holds considerable promise. For example, Qasr Field (discovery announced by Apache in July 2003) is a giant reservoir with more than 2 trillion cubic feet of gas and 50 million barrels of estimated recoverable reserves. Within this broad area, Abdel Fattah [2, 3] recognized that the Matruh Basin (Figure 1) has special importance because of its position with respect to many nearby oil fields. The Matruh Basin was estimated by Shahin [4] to host 23 BBOE with a low attached risk to the preservation of hydrocarbon accumulations because oil migration postdates the severe Late Cretaceous tectonics.

In light of these discoveries and exploration interest, there is a clear need to understand the tectonic history of this area and to define elements of the petroleum system that can lead to continued exploration success. In this paper a thermal model that predicts source rock maturity and hydrocarbon generation for the Matruh Basin and adjacent areas is constructed.

We also use 3D seismic data to illustrate the structural complexity of this area and to help constrain its tectonic history. The study area (Figure 1) covers approximately 5200 square kilometers (≈2085 square miles).

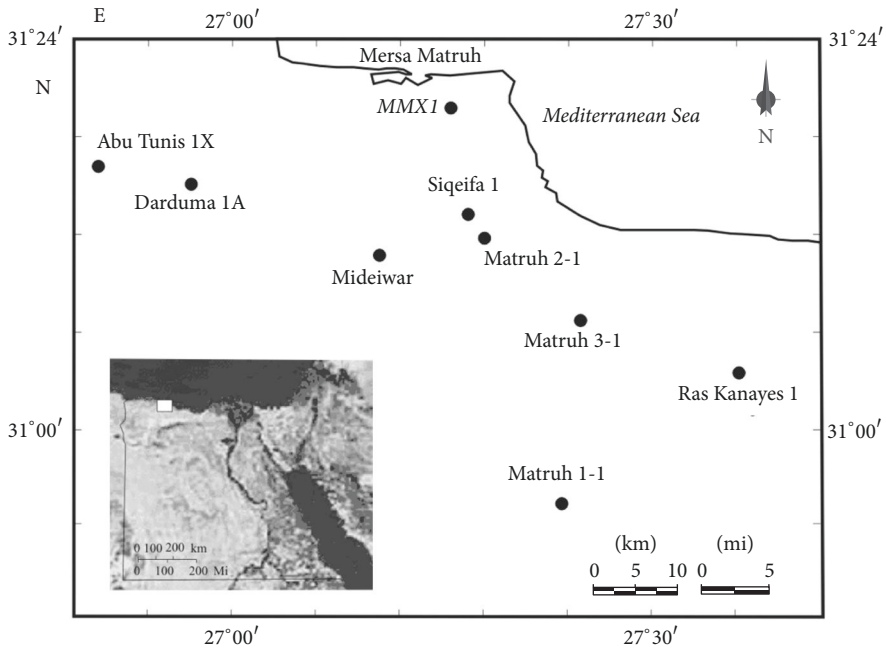

Figure 1: Well location map, Matruh Basin, North Western Desert, Egypt.

The main potential source rocks in the Matruh Basin area are the Lower Cretaceous Alam El Bueib, the Jurassic Khatatba [7], and the Albian Kharita Formations [8]. The hydrocarbon-bearing reservoirs are represented by the Middle Jurassic Khatatba Formation, Lower Cretaceous Alam El Bueib Formation, and the Lower to Upper Cretaceous Bahariya Formation [9]. Three wells, the Alexandrite-1X (2003), Mihos-1X (2004), and Imhotep-1X (2004), lie in the southeastern corner of our study area in the Matruh Basin. They produce gas from the Middle Jurassic Khatatba and Early Cretaceous for Alam El Bueib Formations.

2. Geologic Setting

2.1. Structural Background. The northern part of the Western Desert Basin can be subdivided into five subbasins (Figure 2). The Alamein and Shushan subbasins strike approximately WSW to ENE and are bounded by faults of similar orientation. The Alamein subbasin is bounded to the north by the Dabaa Ridge and to the south by the Alamein Trough. The Shushan subbasin is bounded to the north by the Umbarka Platform and to the south by the North Qattara Ridge. The Qattara subbasin strikes approximately E-W and is bounded to the north by North Qattara Ridge and to the south by the South Qattara Ridge. The Khalda and Matruh subbasins are bordered by NNE to SSW trending faults [5].

The structural evolution of Egypt was influenced by several tectonic events that reactivated older structural trends prevailing in the basement rocks [10, 11]. Hantar [10] identified four main structural trends in the basement rocks, these being orientations of N-S, NE-SW, ENE-WSW, and E-W trends. During the Jurassic, several rift basins were formed as a result of the rifting that was caused by the separation of North Africa/Arabia Plate from European Plate [1]. Following the rifting process, during the Late Cretaceous, the Syrian Arc System was developed due to NW to NNW-SE to SSE compressional forces that affected Egypt as a result of the convergence between African/Arabian and Eurasian plates [12, 13]. This compression lasted into the Eocene and led to the elevation and folding of major portions of the North Western Desert along NE to ENE-SW to WSW trends. Dolson et al. [1] suggested that most of the traps discovered in the Western Desert are related to the Syrian Arc. Starting in the Oligocene and continuing through the Miocene, the rifting of the Gulf of Suez and formation of the Red Sea were fulfilled due to extensional forces in the NE-SW direction [14].

The Matruh and adjacent Shushan subbasins initially may have been formed as a single rift during the Permo-Triassic and later developed in a pull-apart structure [15]. Metwalli and Pigott [7] tested the rifting hypothesis using geochemical data to examine the thermal model. Their results showed that the rifting model approximates reality but that the steady state assumption was not consistent with the geochemical data.

3. Stratigraphy

The complex tectonic history of the Western Desert is responsible for the many unconformities found in the stratigraphy of the area [16]. The sedimentary cover of the North Western Desert ranges in age from Cambrian to Recent [8]. A summary stratigraphic column for the area is shown in Figure 3.

The Mesozoic section is represented by Jurassic and Cretaceous rocks. The Jurassic is composed of three formations. These are, from oldest to youngest, the Wadi El Natrun, Khatatba, and Masajid Formations. The Wadi El Natrun Formation is composed mainly of limestone and shale. This formation is present in the northernmost part of the Western

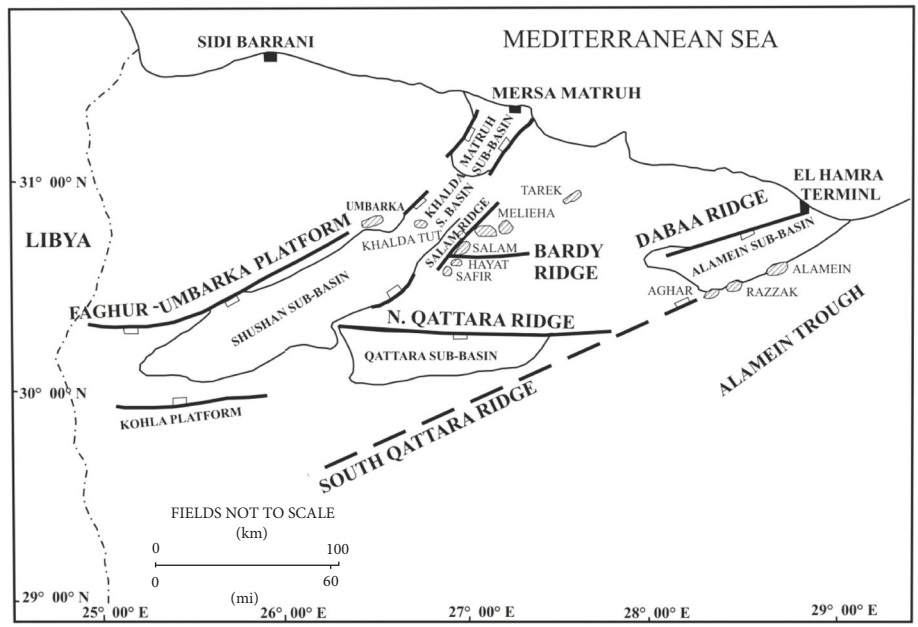

Figure 2: The main five subbasins constituting the Northern Western Desert Basin (after Sultan and Halim [5]).

Desert but undergoes a facies change to its time equivalent Ras Qattara Formation (consisting mainly of sandstones and shales) to the south. In the study area, the Ras Qattara Formation is only presented in the Matruh 1-1 well.

The Khatatba Formation overlies the Wadi El Natrun Formation and is composed of carbonaceous shale with interbedded sandstone and minor thin limestone. The Masajid Formation, composed of limestone with intercalations of shale, conformably overlies the Khatatba Formation.

The Cretaceous system in the Western Desert area has been subjected to various classifications and nomenclatures [8]. As employed here, the Lower Cretaceous system is composed of three formations. The oldest is Alam El Bueib which is a thick succession of clastic rocks deposited unconformably over the eroded surface of the Jurassic Masajid marine carbonates. It is mainly composed of argillaceous sandstones that become shalier toward the northwest [8]. The Alam El Bueib Formation is subdivided into several members, including (1) the Matruh Member (Neocomian, lower Aptian) which is composed of shales and sandstones, (2) the Umbarka Member (Barremian) which consists mainly of sandstone and shale with few streaks of limestone, and (3) the Mamura Carbonate Member which is mainly composed of limestone [17].

The Alamein Formation overlies the Alam El Bueib and is a good regional geological and geophysical marker [8]. It is composed essentially of dolomite and shale. The Kharita Formation overlies the Alamein and is essentially composed of sandstones with thin shale intercalations and rare carbonate interbeds.

The Upper Cretaceous is also represented by three formations: Bahariya, Abu Roash, and Khoman. The Bahariya Formation which is the oldest is composed mainly of sandstone intercalated with shale, siltstone, and limestone [18]. The second formation is the Abu Roash which represents upper Cenomanian/Santonian deposition. This formation is subdivided into seven rock units arranged from top to base as A, B, C, D, E, F, and G and is composed mainly of limestone with minor shale and evaporites. The youngest Upper Cretaceous Formation is Khoman which represents the sediments of Maestrichtian/Campanian. It is mainly composed of limestone.

Tertiary rocks are also present in the area. The Eocene is represented by the Appollonia Formation (lower-middle Eocene) which lies unconformably above the Upper Cretaceous Khoman Formation. It is composed mainly of limestone, occasionally dolomitic, with a few shale layers. The Oligocene-Upper Eocene Dabaa Formation overlies the Appollonia and is mainly composed of shale. The Lower Miocene is represented by Moghra Formation which is composed of sandstone interbedded with shale with few streaks of limestone. The Marmarica Formation, which is the uppermost stratigraphic unit in the area, covers most of the North Western Desert. It was formed during the Middle Miocene and is composed of alternating beds of limestone and shale with some streaks of dolomite.

4. Database and Methodology

Wireline and cuttings logs for nine wells were provided by the Egyptian General Petroleum Corporation (EGPC) and Shell Egypt. The data extracted from the wells were used to construct the burial history, thermal maturity, and lithofacies maps for both the Albian Kharita and the Cenomanian Bahariya Formations (Table 1). The main data required to construct the burial history, subsidence curves, and thermal maturity include formation tops from ground level, absolute time of deposition in millions of years (Ma), lithological composition, hiatus ages, thickness and age of eroded interval, and heat flow data. Absolute age in many of the different

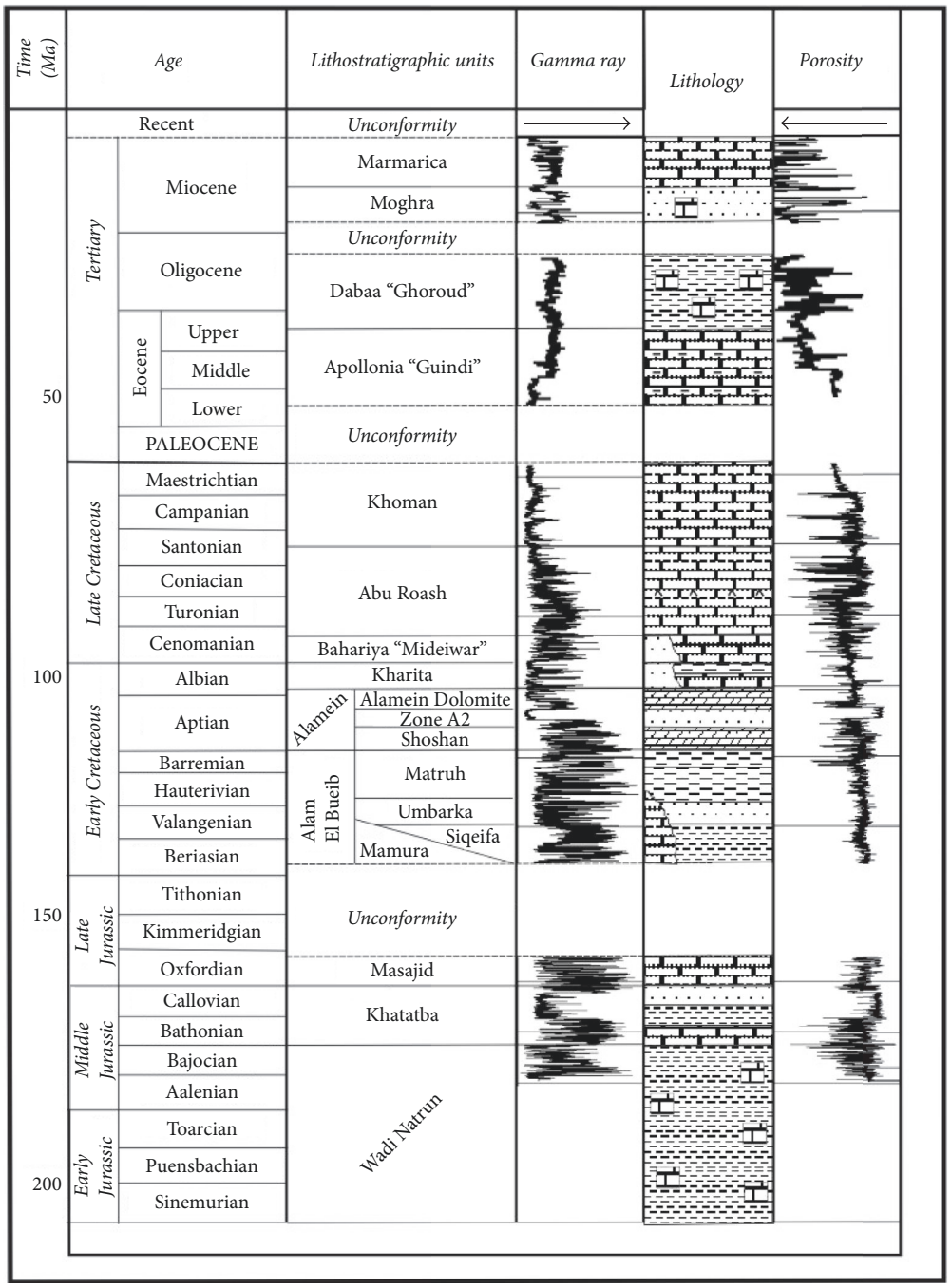

Figure 3: Stratigraphic column of the Matruh area, North Western Desert, Egypt. Modified after MidOil [6].

stratigraphic units was defined using the global stratigraphic chart compiled by Cowie and Bassett [19]. The lithologic composition of the stratigraphic units was obtained from the wireline and cuttings logs.

Two three-dimensional seismic surveys, covering a total area of about 1000 km^2, were provided by Apache Egypt. These data have a 4 s record length, 4 ms sampling rate, and 25 × 25 m bin size. Time slices and vertical transects through amplitude and coherency versions of the data were used to map faults. Detailed structural interpretations of these data will be presented elsewhere. In this paper the discussion of the seismic data is restricted to illustrating the types of structural features present in this area that cannot be observed or adequately mapped using well control alone and relating these features to the results of our subsidence history analyses.

The net subsidence in a basin results from the combination of both subsidence due to tectonics and subsidence owing to sediment and water loading. The process used to determine the amount of load induced subsidence is isostatic backstripping. This method removes sediment layers,

Table 1: Lithologic constituents of Bahariya and Kharita Formations. Matruh Basin, North Western Desert, Egypt.

Formation name	Lithology							Well name
	% SS	% LS	% Anh.	% shale	% SiltSt.	% Dolom.	% clay	
Kharita	72.3	11.4	0.4	10.9	0.5	4.5		Darduma 1A
Bahariya	40.8	24.2		27.4	3.3	2.1		
Kharita	60.2	4.2		31.6		4		Siqeifa 1X
Bahariya	33.4	28.3		34.6		3.7		
Kharita	69.5	3.2	0.7	21.7		4.5		Mideiwar 1X
Bahariya	47.3	20.5		25		7.2		
Kharita	69.4	1.4	1.1	23		5.1		Abu Tunis 1X
Bahariya	46.7	18.2	0.1	24		11		
Kharita	71.8	2.4		18.5		7.3		Marsa Matruh MMX-1
Bahariya	28.9	31.6		38.7			0.8	
Kharita	68	1.1		22.1	8.2	0.6		Matruh 1-1
Bahariya	53.7	13.2		33.1				
Kharita	72.7			21.4		5.9		Matruh 2-1
Bahariya	27.7	22.8		42.2		7.3		
Kharita	69.7	3.9		23.2		3.2		Matruh 3-1
Bahariya	24	16.2		50.9		8.9		
Kharita	78.3	0.8		18		2.9		Ras Kanayes Ja27-1
Bahariya	36.2	16.2		47.6				

correcting for decompaction, fluctuation of sea level and sea depth and, assuming Airy isostasy, adjusts for isostatic compensation. Tectonic subsidence is basement involved and occurs by an observable time transient change in lithospheric thickness, with accompanying perturbation and change in the crust's thermal state [7].

Temperature is the most sensitive parameter in hydrocarbon generation. Thus reconstruction of temperature history is essential when evaluating petroleum prospects [20]. Petroleum generation is temperature-dependent and time-dependent but varies exponentially with temperature and linearly with time [21]. The temperature and time dependency for hydrocarbon generation are described by the Arrhenius equation:

$$K = A \exp^{(-E_a/RT)}, \quad (1)$$

where K is the rate constant; A is the frequency factor; E_a is the activation energy; R is the Gas constant (Joule mole^{-1} K^{-1}); and T is the absolute temperature (°K).
The Arrhenius equation suggests that 10°K rise in temperature causes the reaction rate to double.

The BasinMod 1D software (Platte River Associates) was used in this study for modeling both the basin subsidence and consequent hydrocarbon potential of the available boreholes.

5. 3D Seismic Structural Analysis

Harding (1985) stated that "early identification of structural style is an important exploration function and the appropriate selection of prospect (trap) models often depends on the reliability of such identification."

6. Faults Characteristics and Interpretation

Matruh Basin is highly faulted. The faults affecting the time zone of interest (~800–1500 ms) were interpreted first in order to reveal the geologic history of the area and allow horizons to be correctly correlated as well as help in predicting what sort of hydrocarbon traps may be exist in the area. The fault interpretation was carried out through the interpretation of the vertical transects through the amplitude volume resulted from the poststack processing techniques applied as well as the time slices through the coherency volume.

The time slices through the coherency volume (Figures 4 and 5) reflect that all faults strike NW-SE. Consequently, to interpret these faults, a series of 21 equally spaced vertical transects extending NE-SW (perpendicular to the faults direction) were interpreted. The location map of the seismic line used in the interpretation of faults is given in Figure 6.

Figures 7–9 illustrate vertical transects with the interpreted faults, while Figures 10 and 11 show picked faults on the uninterpreted time slices (Figures 4 and 5) at 1000, 1200, 1400, and 1600 ms through the coherency volume.

Generally, all the interpreted faults through the seismic volume are extensional normal faults that generally form grabens and half grabens that extend throughout the study area. The length of these faults planes varies from more 9 Km to minor faults with lengths of about few hundreds of meters. Their vertical extension (in the time direction) varies from approximately 200 ms to major faults of about 2700 ms. In terms of fault mechanical stratigraphy, note that there are at least two distinct episodes of extension revealed by two fault populations: those who terminate below the ~110 ma Alamein and those that terminate and cut the ~90 Abu Roash. As Pigott and Abouelresh [22] have pointed out, owing to

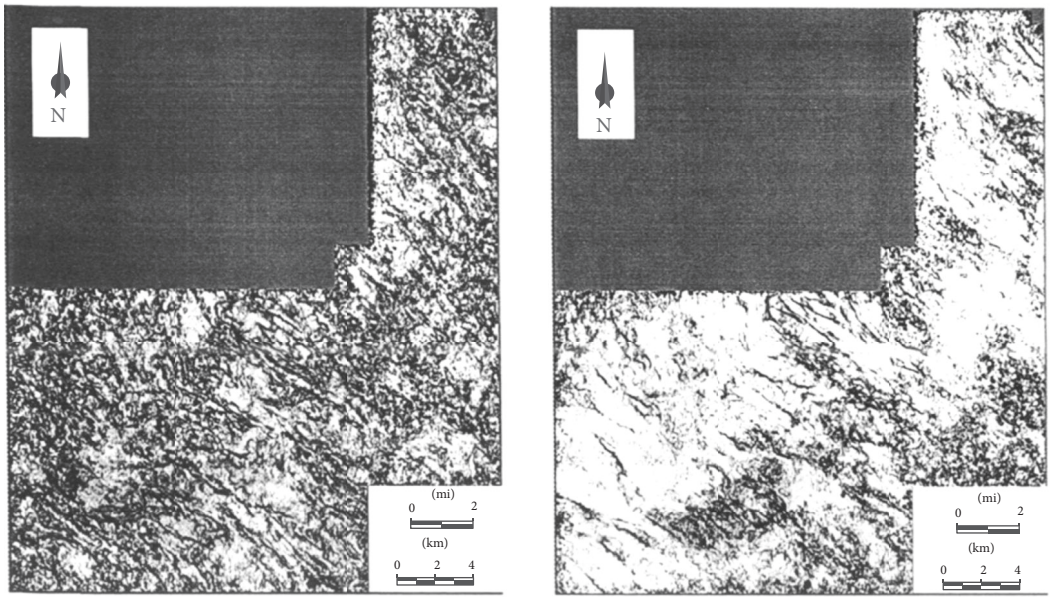

(a) (b)

Figure 4: Time slices at 1000 ms through the coherency volume for *Upper Bahariya Formation* (a). Time slices at 1300 ms through the coherency volume for *Kharita Formation* (b).

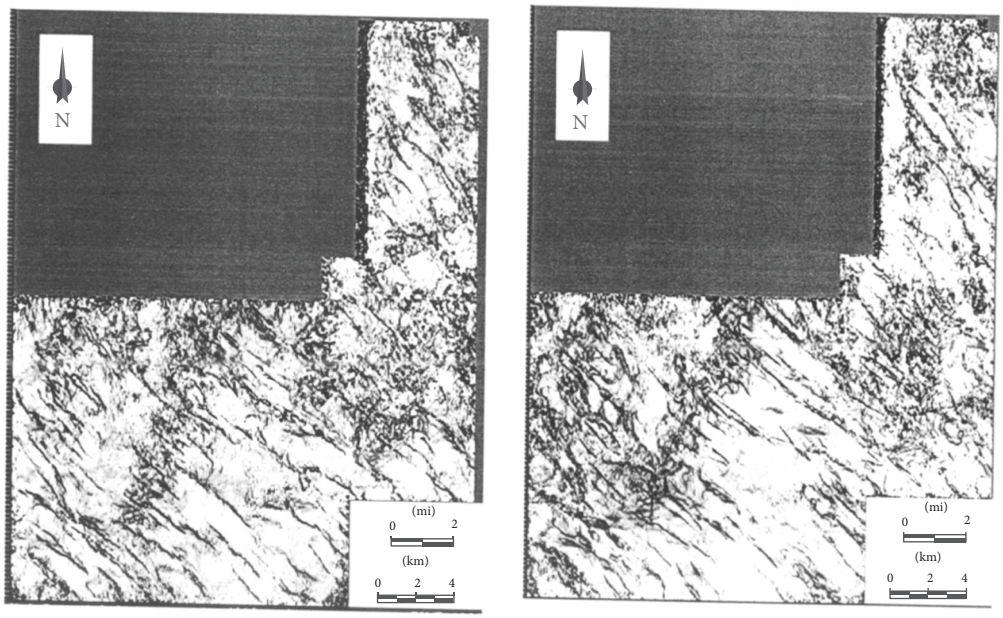

(a) (b)

Figure 5: Time slices at 1400 ms through the coherency volume for *Base Kharita Formation* (a). Time slices at 1600 ms through the coherency volume for *Alam El Bueib 1 Formation* (b).

the general increase in bulk modulus with increasing depth of overburden, deep seated faults rupture young rocks but extension of young rocks will not rupture deeper rocks. Thus, the upper fault termination provides the youngest age of Page 18 of 40 a fault. Therefore, for these seismic observations in the Matruh Basin, the fault mechanical stratigraphy reveals a pre-Alamein and a post-Abu Roash time of extension. As we shall see later in this paper, these two extension events are confirmed by the 1D basin subsidence analysis.

The structure contour maps of both Bahariya and Kharita Formations are shown in Figure 12. Those maps show that the tops of the two formations dip to the southeast to reach their deepest values, at the Ras Kanayes well, reached 5711 ft (1741 m) for Bahariya and 6717 ft (2047 m) for Kharita. The

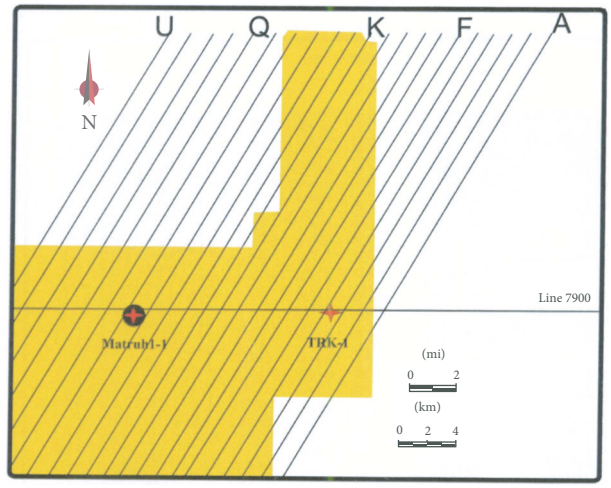

Figure 6: Location map of the equally spaced lines used in the interpretation of faults.

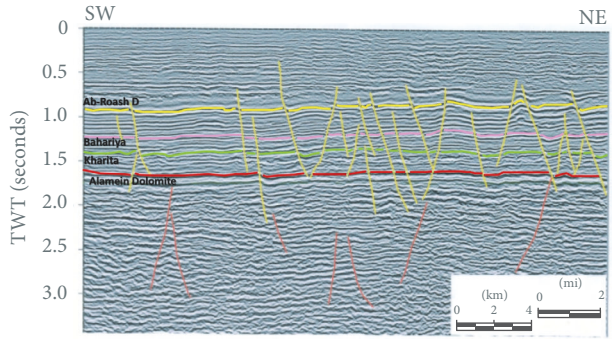

Figure 7: Interpreted seismic line number "F" (see Figure 6 for location).

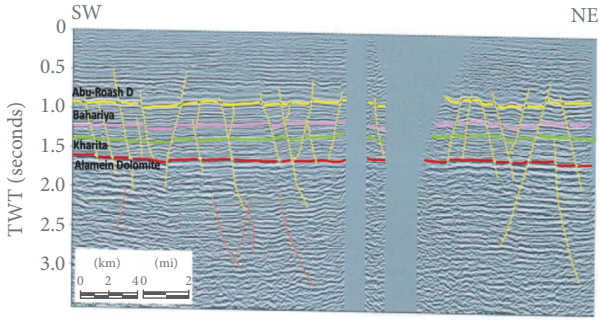

Figure 8: Interpreted seismic line number "K" (see Figure 6 for location).

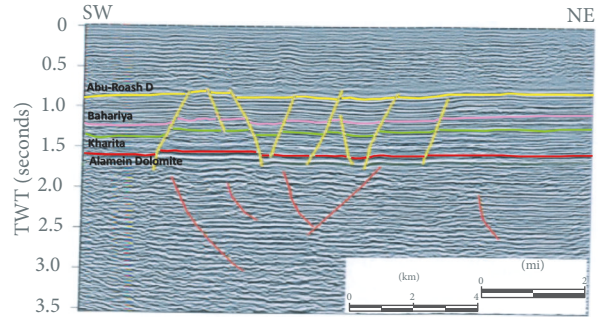

Figure 9: Interpreted seismic line no. "Q" (see Figure 6 for location).

shallowest values for Bahariya and Kharita Formations are recorded at the MMX-1 well with values of 3823.6 ft (1165 m) and 4689 ft (1429 m), respectively.

Figure 13 shows a structure map of the Alamein Dolomite that was based on the data from the nine well and a depth-converted Alamein Dolomite horizon that was picked in two 3D seismic volumes (grey area). The map shows a general dipping trend to the southeast direction of the area under consideration to exceed the depth of 8700 ft (2651.8 m) at the south east corner. As shown in Figure 5(a), enormous number of faults is affecting the area. Generally, these faults strike NW-SE and are extensional normal faults that generally form grabens and half grabens. While Figure 5(b) shows a sequence of Syrian Arc folds with axial surfaces that

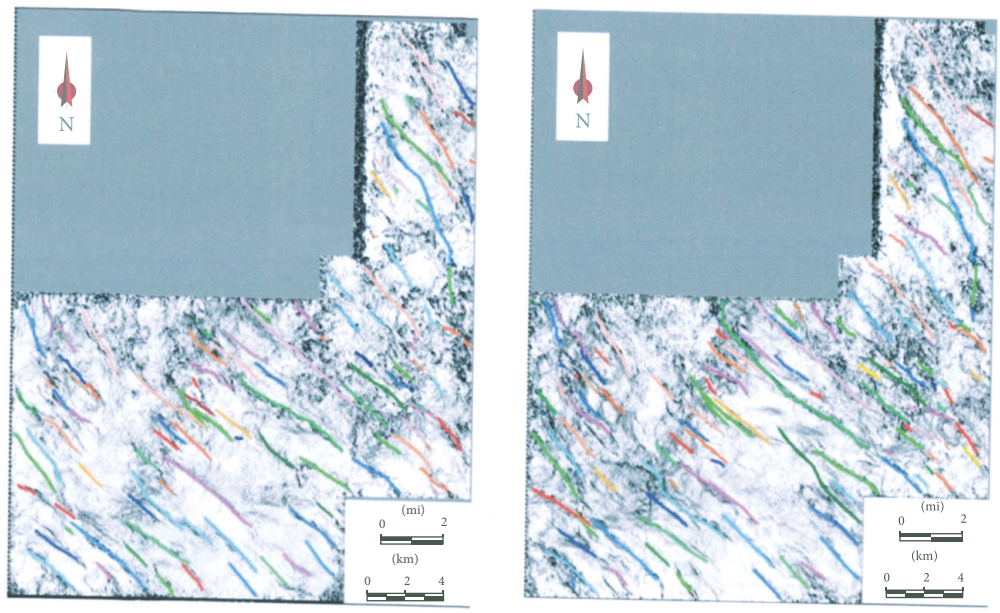

(a) (b)

Figure 10: Tracked faults on coherency time slice at time 1000 ms. For *Upper Bahariya Formation*, (a) the uninterpreted time slices on Figure 4(a). Tracked faults on coherency time slice at time 1200 ms. For *Kharita* Formation, (b) the uninterpreted time slices on Figure 4(b).

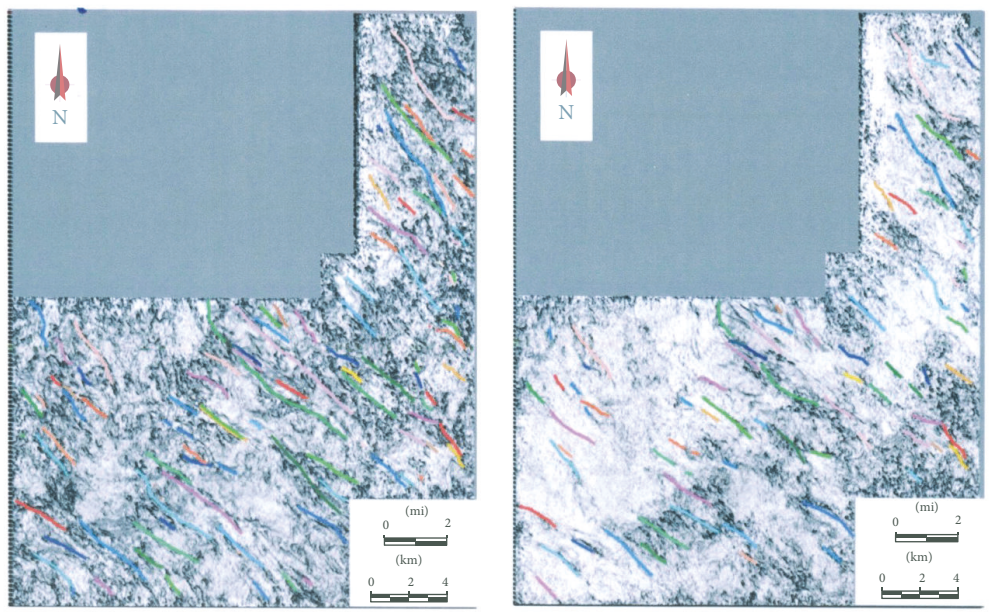

(a) (b)

Figure 11: Tracked faults on coherency time slice at time 1400 ms. For *Base Kharita* Formation, (a) the uninterpreted time slices on Figure 5(a). Tracked faults on coherency time slice at time 1600 ms. For *Alam El Bueib 1 Formation*, (b) the uninterpreted time slices on Figure 5(b).

strike NE-SW. These structures may have been formed at Santonian/Campanian times.

Comparison of Figure 13, which incorporates 3D seismic data, with the structure maps shown in Figure 12 clearly indicates that not all of the structural elements present in this area are being captured using well control alone (i.e., all of Figures 12(a) and 12(b) and part of Figure 13). As described below, lithofacies and isopach maps were constructed from the available well control. As the sparse well control is unlikely to capture all the changes in lithology and thickness within the study area, nevertheless, the broad-scale trends (e.g., regional structural dips and thickness changes) are being

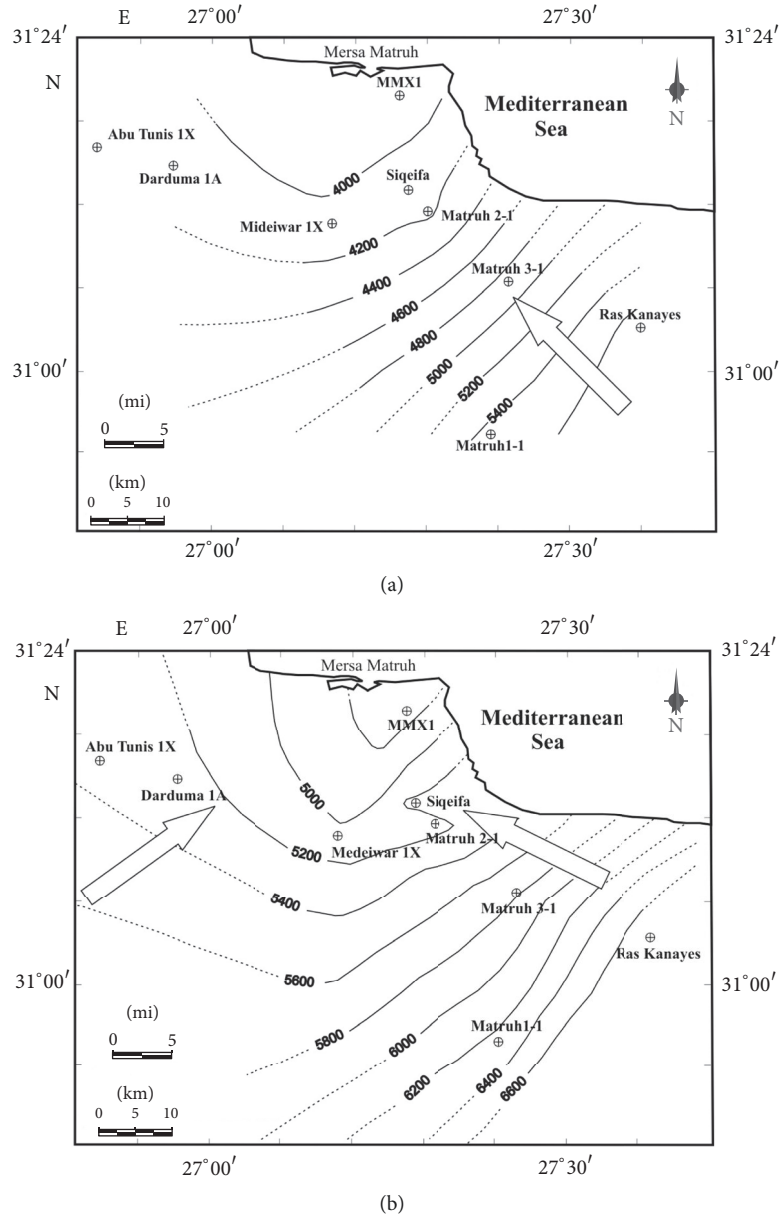

Figure 12: Structure contour maps of Bahariya (a) and Kharita (b) Formations. Arrows refer to the possible hydrocarbons migration pathway.

sufficiently well defined using well control to warrant use of the maps for subsequent analyses presented in this paper. Furthermore, in the absence of other published data, we hope that the analyses presented here will be of use to explorationists working this area.

7. Lithofacies Analysis

The sand to shale ratio maps of Bahariya and Kharita Formations are illustrated in Figures 15(a) and 5(b), respectively. The Bahariya (Figure 15(a)) shows an increase in sandstone to the west, with shale being dominant in the eastern parts of the area. The Kharita map (Figure 15(b)) shows a lowest value at Siqeifa 1X well (1.9) and an increase to both the east and west. The highest sand to shale ratio (6.6) for this formation is in the Darduma 1A well. Although sandstone and shale are the two main lithologic constituents in the Bahariya and Kharita Formations, Table 1 shows that other lithologies are also present and can be important constituents. For example, approximately 31% of the Bahariya Formation consists of limestone in the MMX-1 well.

The isopach maps of Bahariya and Kharita Formations are shown in Figures 16(a) and 16(b), respectively. Both maps demonstrate a general increase in thickness to the northwest direction, reaching maxima in the Darduma 1A well, which penetrated 1182.1 ft (360.3 m) of the Bahariya and 2305 ft

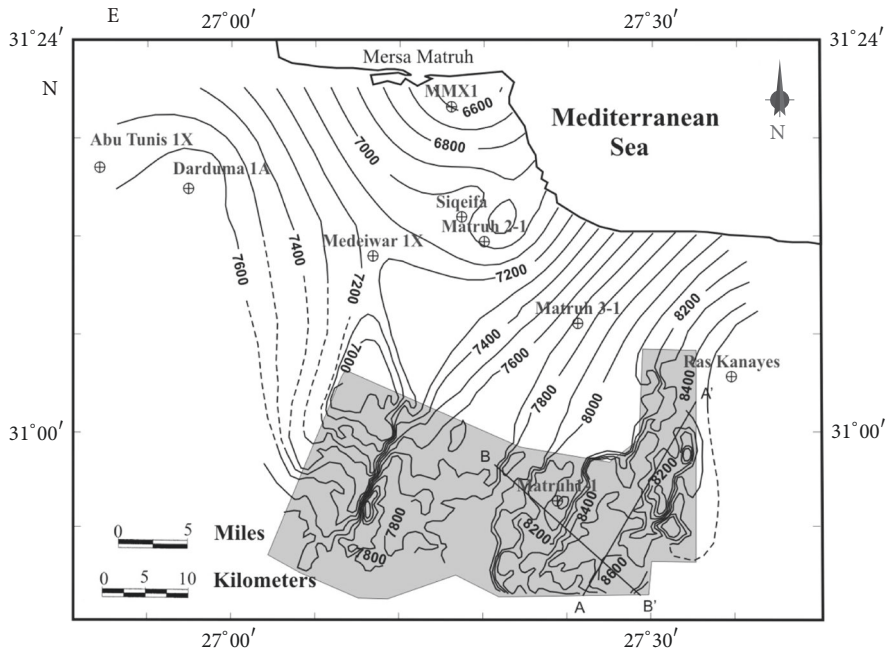

Figure 13: Structure contour map of Alamein Dolomite Formation. A-A′ and B-B′ are locations of the seismic sections in Figure 14.

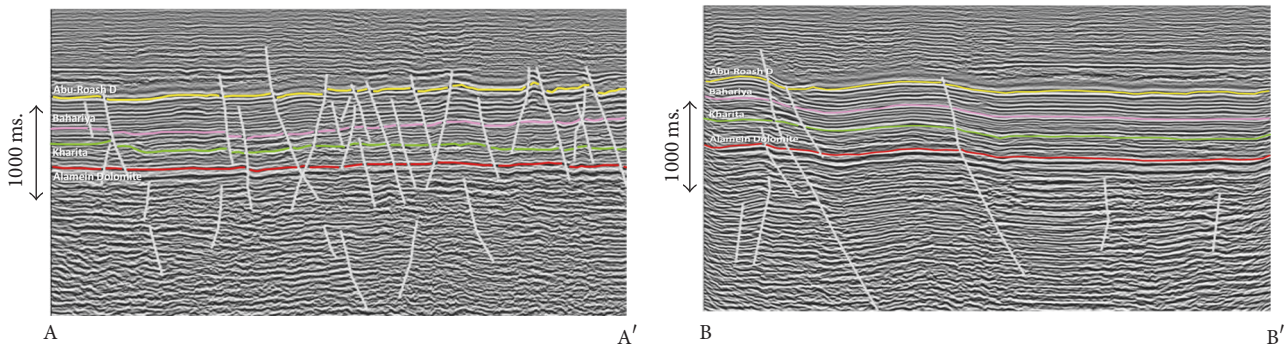

Figure 14: Sample seismic vertical transects showing enormous amount of faults trending NW-SE (a) and Syrian Arc folds (b). Locations of these transects are shown on Figure 13.

(702.6 m) of the Kharita Formation. The lowest value for each of the two formations is recorded at Matruh 1-1 with a value of 794 ft (242 m) for Bahariya and 1158 ft (352.9 m) for Kharita.

Unfortunately, similar to the structure maps constructed without 3D seismic control, these isolith and isopach maps are unlikely to capture all of the stratigraphic variability present in the area. The maps are presented as they help to put first-order controls on the petroleum system of this area.

8. Burial History and Subsidence

The quantitative analysis of burial history through time is used to reconstruct thermal and maturity histories. This analysis aims at producing time depth histories and sedimentation rates. The correction of decompaction needs to be carried out for burial history analysis. Decompaction (backstripping) is based on the skeletal (solid grain) volume being constant while the rock volume is changed with depth of burial due to the loss of porosity [23].

Figure 17 shows the burial history and subsidence curves in the Darduma 1A, Mideiwar 1X, Matruh 1-1, and Ras Kanayes wells. These figures indicate a rapid subsidence during the Late Jurassic Early Cretaceous times. The fault mechanical-dominated subsidence (when highest tectonic subsidence rate) is represented by the steep part of the burial history diagram. The slope of the burial history curves change at time intervals which corresponds to the Turonian (92 Ma) and become flatter, indicating the dominance of crustal thermal cooling subsidence. Uplift can also be noticed in all the wells that started at the Cretaceous/Paleogene (73 Ma).

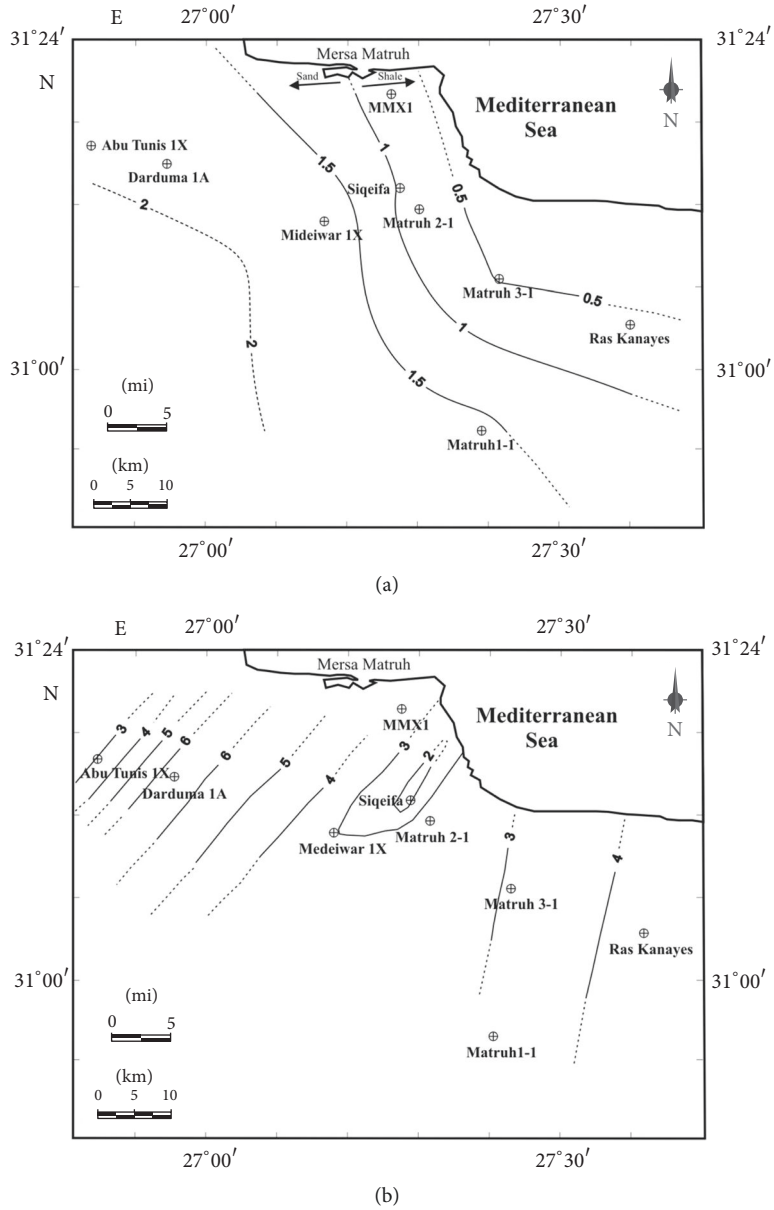

Figure 15: Sand to Shale ratio maps of Bahariya (a) and Kharita (b) Formations.

This uplift may be as a result of the Syrian Arc that caused inversion in most of North Western Desert Basins [1, 12, 24].

9. Thermal History and Source Rock Maturity

Ghanem et al. [8] evaluated the potential source rocks of the Lower Cretaceous rocks in the Matruh Basin in a study that was based essentially on the geochemical analysis of these sediments. They concluded that the Kharita Formation is a fair to good source rock.

An application of Arrhenius relationship is the Time-Temperature Index (TTI) [25, 26]. This index is based on the view that the reaction rates double every 10°C rise in the temperature.

In the current study the bottom hole temperatures that were corrected to the cooling effect were used to construct the thermal history applying the rifting heat flow approach. The beta factor (β_{init}) is the ratio of the lithospheric thickness immediately after stretching to the initial lithospheric thickness. Figure 18 shows the β_{init} factor map of the study area which shows values to range from 1.1 to 1.7 with the values increase to the southeast direction toward the deeper parts of the basin.

Figure 19 shows the burial history and maturity profiles which reveal the Albian Kharita Formation and Cenomanian Bahariya Clastics to be in the early to middle maturity levels. A representation of the maturity prediction versus depth is shown in Figure 20. The figure shows that the early

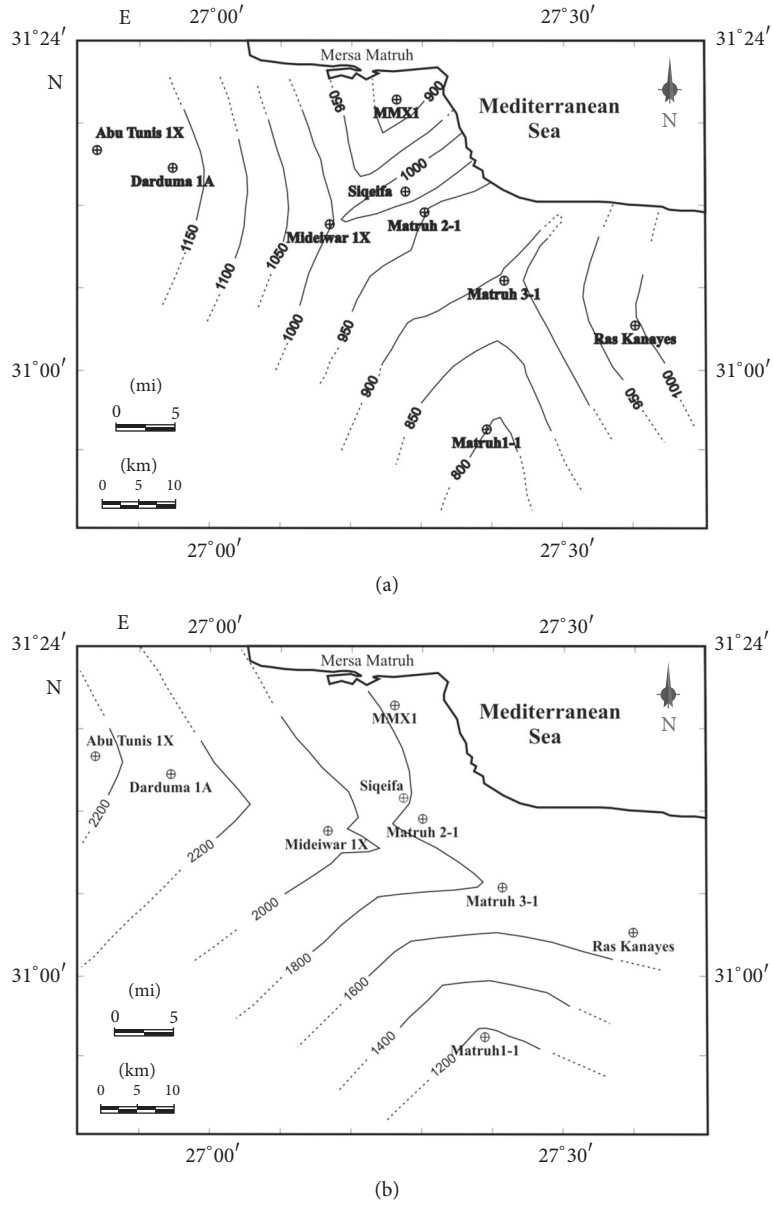

Figure 16: Isopach maps of Bahariya Formation (a) and Kharita Formation (b).

maturation (R_o = 0.5 percent) started almost at a depth of 2800 ft (853.4 m) at Ras Kanayes to 3000 ft (914.4 m) at Mideiwar 1A while the main gas started at approximately 7700 ft (2346.9 m) at Darduma 1A to 9000 ft (2743.2 m) at Matruh 1-1.

Figure 21 shows a maturity depth map which shows the depth to the top of the oil window (Ro = 0.55). It shows a general decrease in the maturity depth values to the southeast direction of the area.

10. Discussion and Results

The sand to shale ratio map of Bahariya (Figure 15(a)) reveals sandy facies in the western parts and shaly facies in the eastern parts of the study area. The Kharita shown in Figure 15(b) reveals a primarily sandy formation, and it has some shale volume that can enable Kharita to be a significant source rock. Bahariya serves as a primary reservoir in the Matruh Basin. The presence of these shale ratios in Bahariya will work as a lateral seals that increase (together with the impermeable cover of Abu Roash Carbonates and Shales) its reservoir abilities.

It was indicated from both stratigraphic and seismic interpretation and the geology review of the North Western Desert that the Matruh-Shushan basins were formed in the Middle-Late Jurassic as a rift basin [7].

McKenzie [27] classically described a procedure for the formation of extensional rifting basins through which subsidence occurs in two stages:

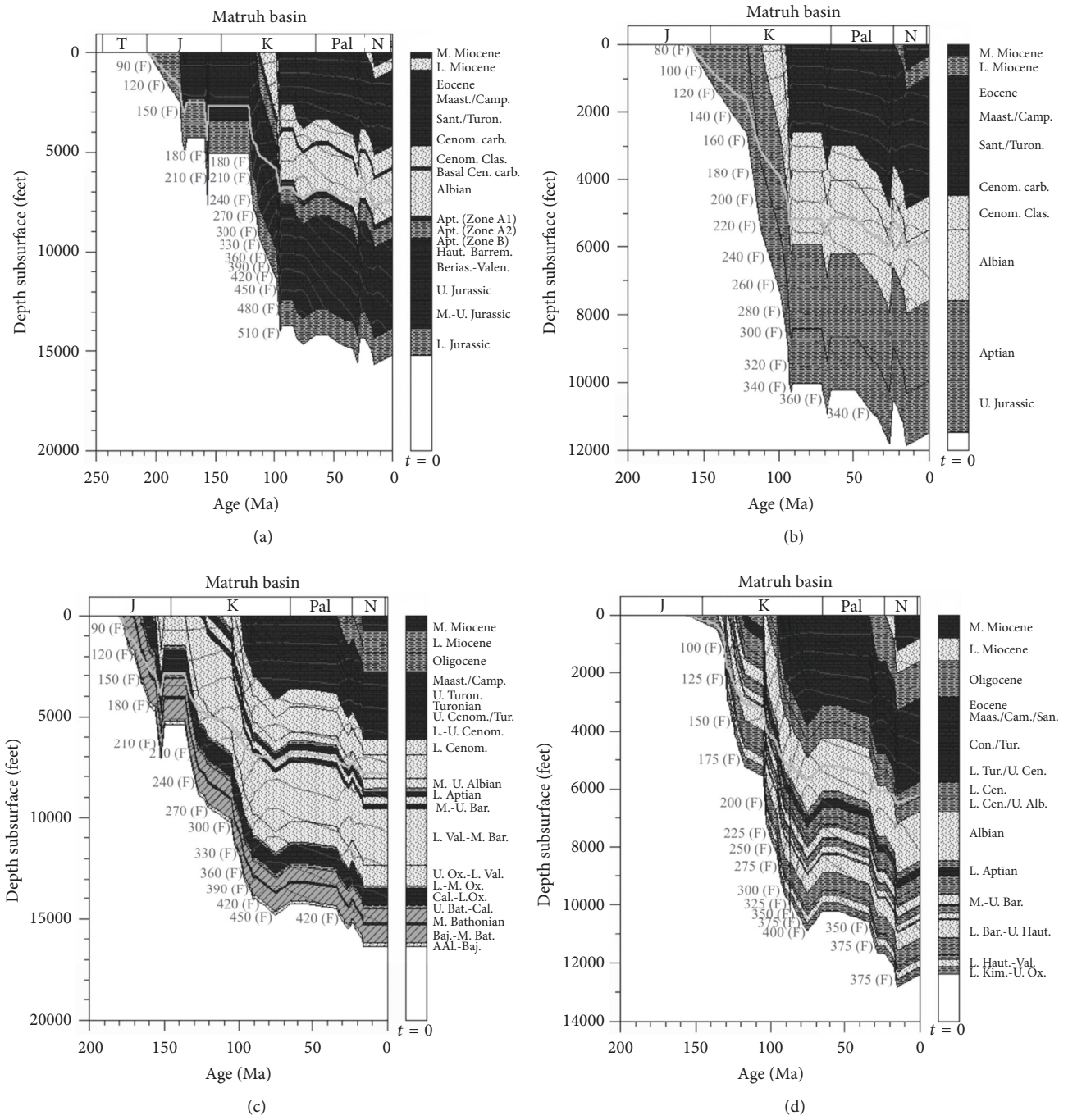

Figure 17: Burial history profiles, subsidence curves, and the isotherms for the wells Darduma 1A (a), Mideiwar 1X (b), Matruh 1-1 (c), and Ras Kanayes (d).

(i) First stage is the tectonic subsidence results by stretching of the lithosphere by extensional forces. This stage is accompanied by upwelling of the hotter asthenosphere which worms up the lithosphere.

(ii) Second stage is the thermal subsidence as a result of the cooling of the lithosphere. This subsidence takes place through a longer time than the first one.

Figure 17 indicates two *distinct episodes of* rapid subsidence: one during the Late Jurassic Early Cretaceous (pre-Alamein) time and one during the post-Abu Roash Middle Cretaceous. The fault mechanical-dominated subsidence (when highest tectonic subsidence rate) is represented by the steep part of the burial history diagram. The slopes of the burial history curves change at time interval which corresponds to a ~160

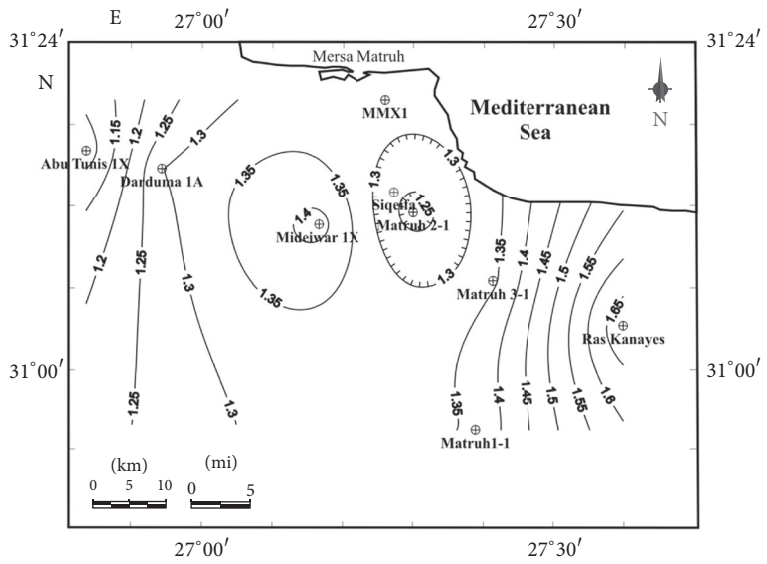

Figure 18: Stretching (β_{init}) factor map of the study area.

pre-Alamein event and a younger than Turonian (92 Ma) post-Abu Roash event. Note that the 1D basin subsidence model events are confirmed by the previously mentioned two episodes of faulting. In both cases, during rifting, the top of the asthenosphere moves to much shallower depths leading to higher heat flows and higher geothermal gradients with values which will depend on how much the crust is thinned and this is conveniently expressed by the β_{init} "stretching factor" introduced by Metwalli and Pigott [7]. Thus, it is defined so that the larger the number the greater the lateral extension [21]. From these two extension events, the depth to the oil window (Figure 21) decreases to the southeast direction, the same direction of the increase of the stretching β_{init} factor (Figure 18) as well as the increase in the shale percentages in the source Kharita Formation.

As shown previously, Kharita and Bahariya Formations are thermally mature enough for hydrocarbon generation. The maturation levels at the surface of the Bahariya, Kharita, and Alamein (lower surface of Kharita) can be shown in Figures 22–24. Figure 22 shows that, in the northwest half of the area, Bahariya is in the early mature stage, while it is in the mid mature stage in the southeast half of the area. The major parts of Kharita Formation (Figure 23) are in the mid mature stage except for these narrow areas in the north (at well MMX1) and to the west (at Abu Tunis 1X well) which are in the early maturation level. Finally, the maturity levels have increased through the thick body of Kharita Formation to reach the main gas generation at the well (Darduma 1A) and mid maturation levels to the northeast and northwest of the area and late maturation levels at the rest parts of the area. The generated hydrocarbons will migrate in the directions of the arrows shown on the structure contour maps of Bahariya and Kharita (Figures 12(a) and 12(b)) to the higher level at the direction of the well MMX-1 in which Bahariya has higher shale and limestone percentages (Table 1) that can work as lateral seals in addition to the impermeable limestone cap rock of Abu Roash Formation. Caution should be taken as the area is highly faulted and structurally complicated as can be seen on the sample seismic transects in Figures 14(a) and 14(b) that shows the opportunity of having hydrocarbon traps at such relatively shallow level through the faults (Figure 14(a)) and/or Syrian Arc anticlines (Figure 14(b)).

11. Conclusions

Matruh Basin, as a rift basin, exhibited a rapid subsidence during Middle and Late Jurassic which continued during the early Cretaceous. This subsidence was followed by a thermal subsidence that started approximately at the Turonian (92 Ma).

The Albian Kharita Formation showed a sandy facies with a considerable volume of shale that enables it to be a good source rock. A high percentage of shales in Kharita Formation and high sealing efficiency have been responsible for the concentration of gas and condensate in the Albian sourced Kharita sandstones, rather than in the higher, younger formations. Bahariya Formation can be a considerable source rock especially in the shaly portions to the east of the study area.

Due to transitional facies characters, shale occurrence tends to be localized and shale/sandstone vertical ratios tend to vary in the different formations. The best sealing conditions are said to occur in the basinal areas rather than on ridge/platform areas, where sequence becomes more sandy.

The constructed thermal models show that the Albian Kharita and Cenomanian Bahariya deposits in the Matruh Basin are mature enough to produce hydrocarbons. While Bahariya showed an early maturation levels to the northwest

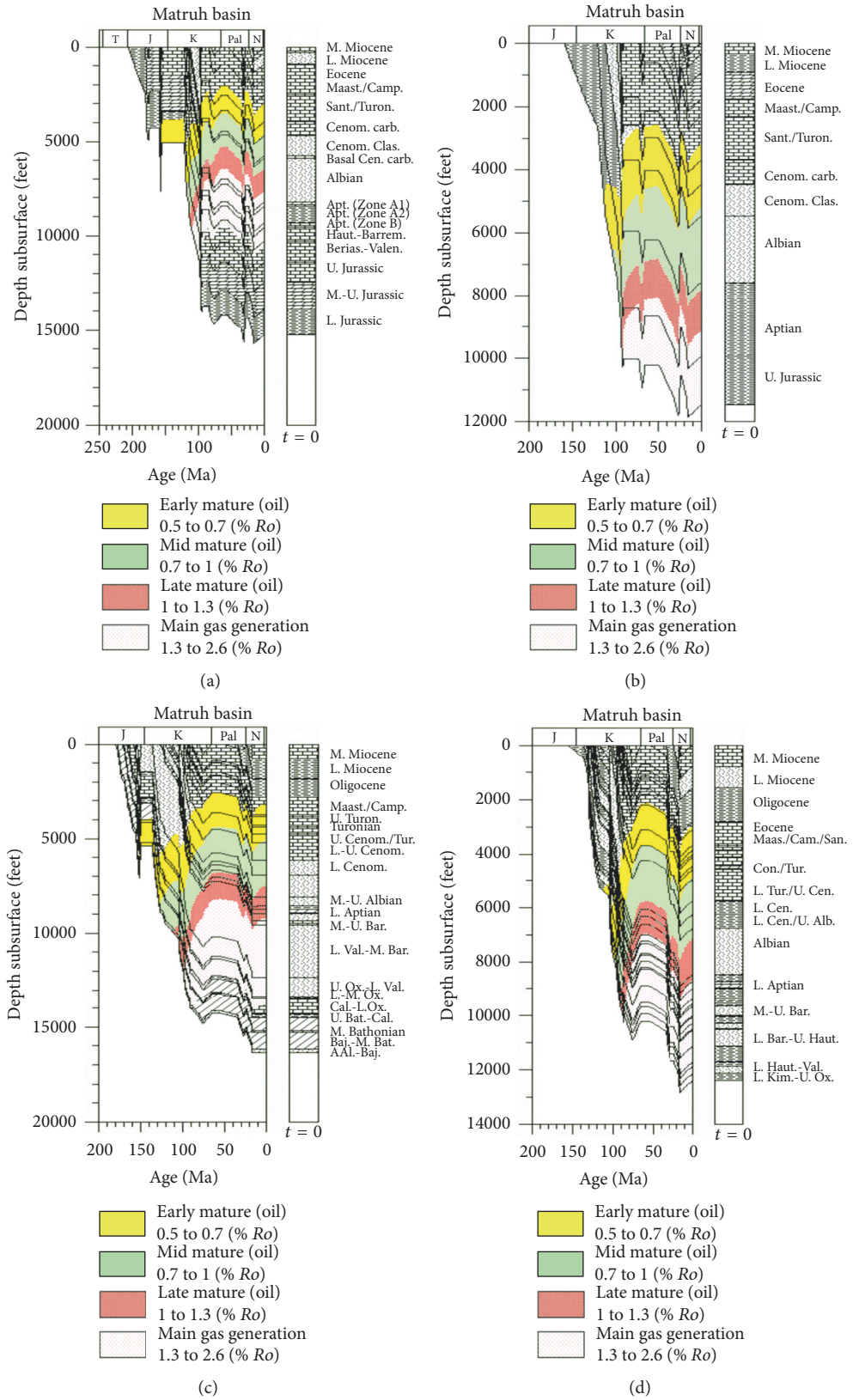

Figure 19: Burial history profiles and maturity windows for the wells Darduma 1A (a), Mideiwar 1X (b), Matruh 1-1 (c), and Ras Kanayes (d).

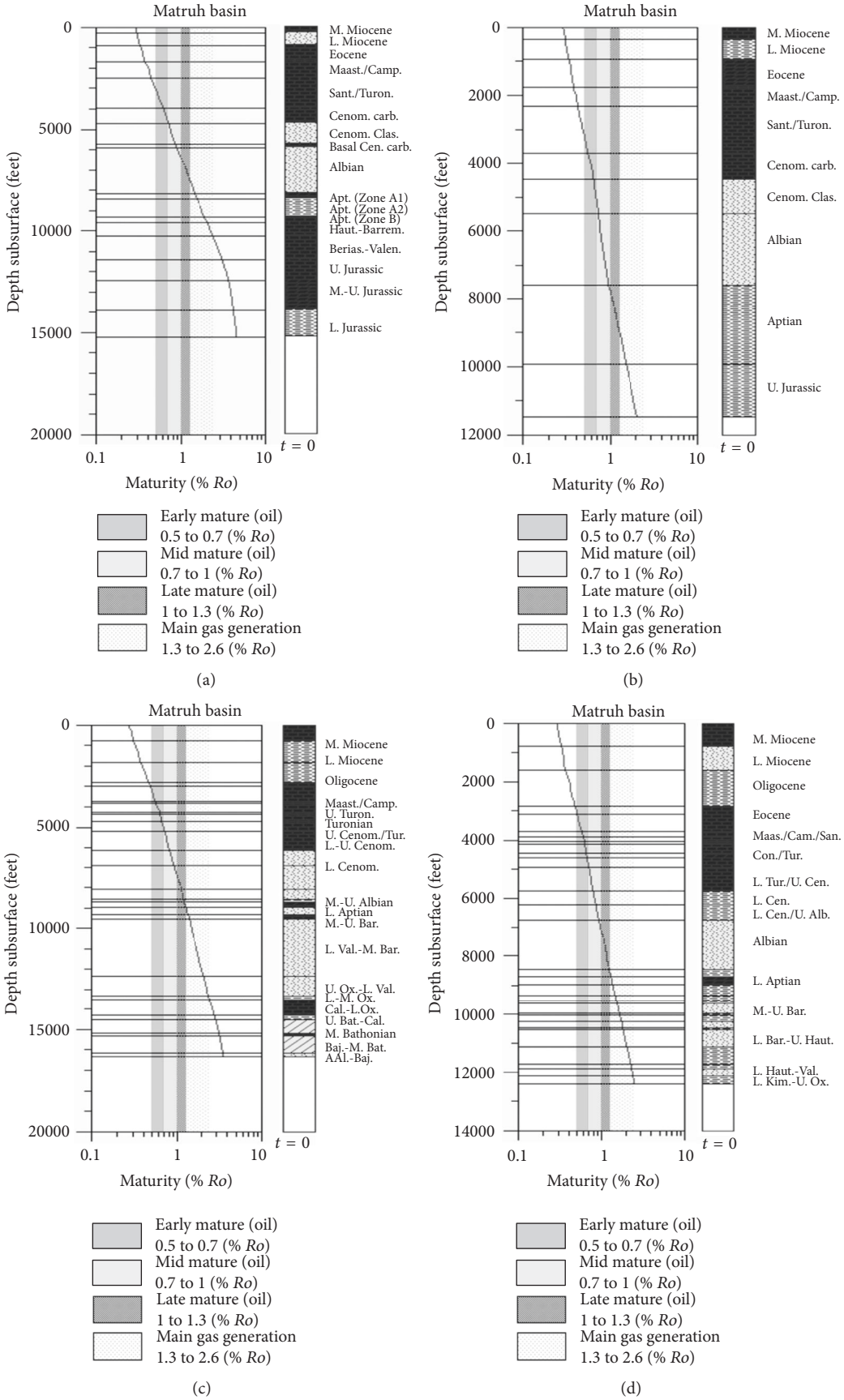

Figure 20: Maturity profiles for the wells Darduma 1A (a), Mideiwar 1X (b), Matruh 1-1 (c), and Ras Kanayes (d).

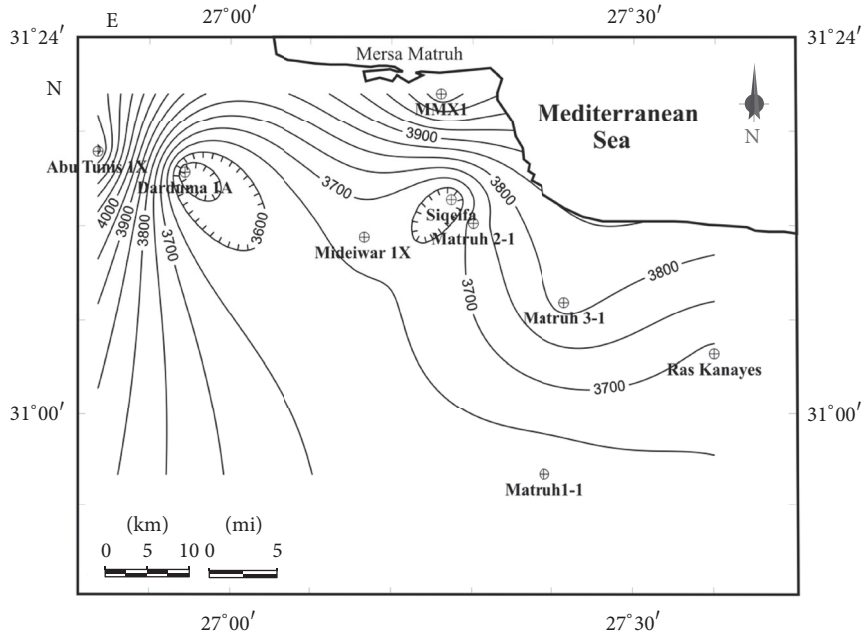

Figure 21: Maturity depth map of the study area.

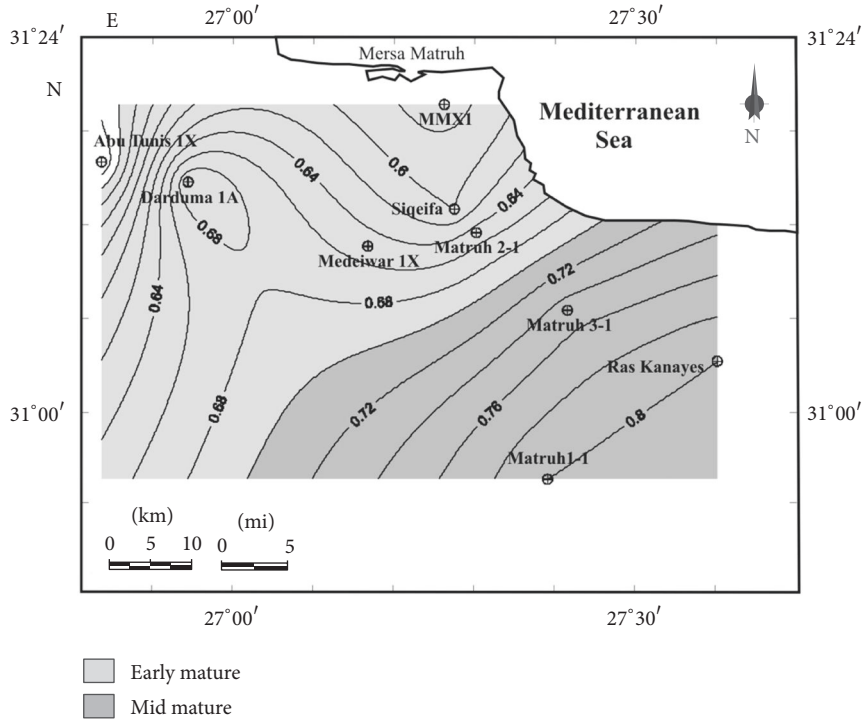

Figure 22: Maturity levels at the surface of Bahariya Formation.

and mid maturation to the southeast, Kharita showed mid maturation levels in the most parts of the area. These thermal models are concordant with the discovered gas reservoirs in the Matruh Basin from the deeper Alam El Bueib and Khatatba Formations. This work suggests that oil and gas discoveries can be fulfilled in the shallower levels of the Matruh Basin. That will require a detailed structural analysis at these levels.

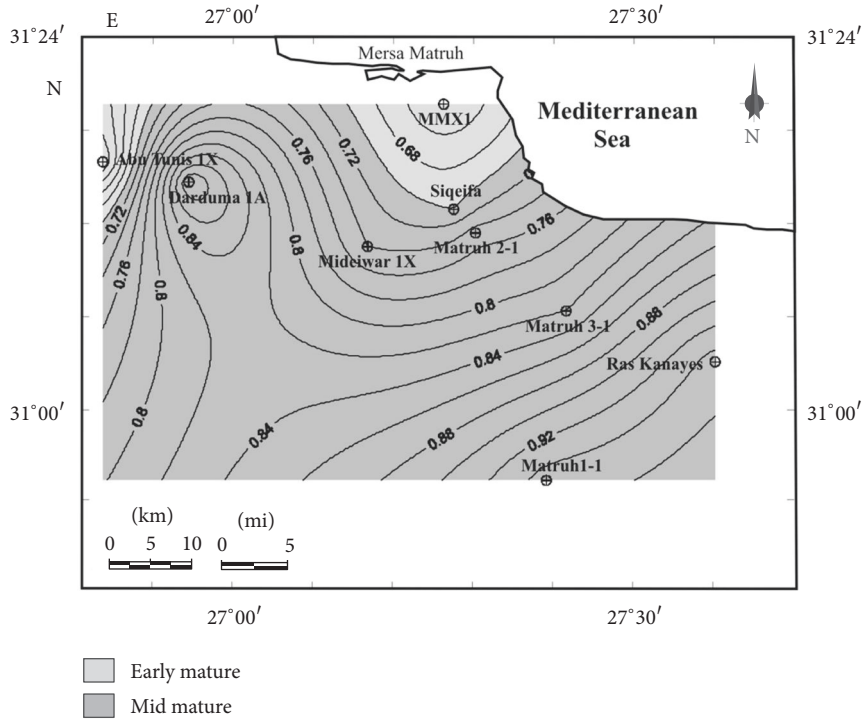

Figure 23: Maturity levels at the surface of Kharita Formation.

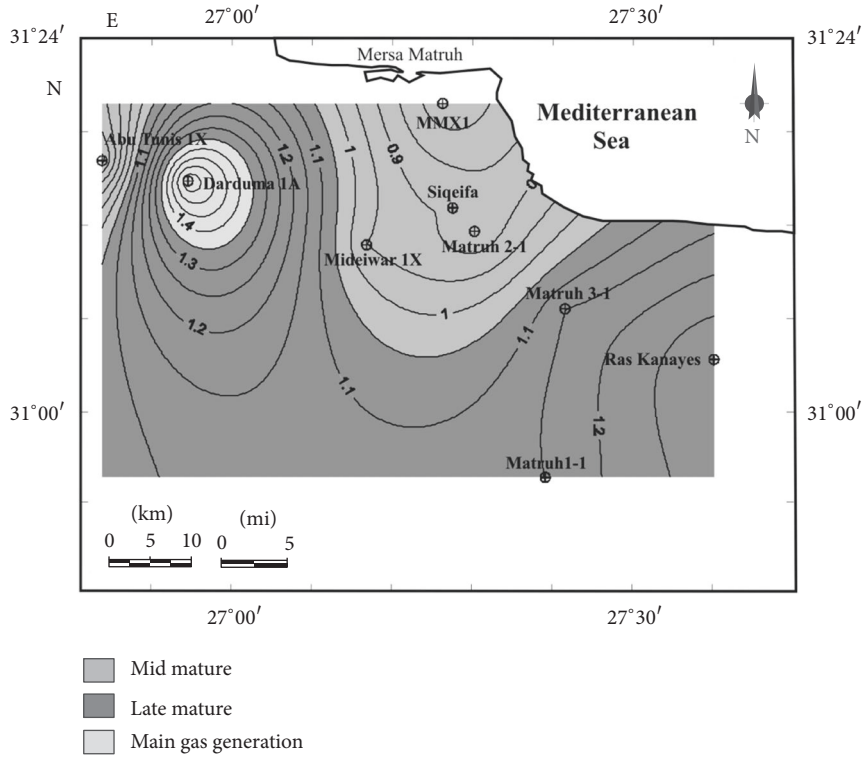

Figure 24: Maturity levels at the surface of Alamein (lower surface of Kharita) Formation.

Conflicts of Interest

The authors declare that they have no conflicts of interest.

References

[1] J. C. Dolson, M. V. Shann, S. Matbouly, C. Harwood, R. Rashed, and H. Hammouda, "The Petroleum Potential of Egypt," in *Petroleum Provinces of the 21st Century v. Memoir 74*, W. A. Morgan, Ed., pp. 453–482, American Association of Petroleum Geologists, Tulsa, Okla, USA, 2001.

[2] T. Abdel Fattah, "Petrophysical geological and geophysical studies at Matruh basin," *Qena*, vol. 1, no. 2, pp. 61–74, 1993.

[3] T. Abdel Fattah, "Source rock evaluation of the pre-Aptian section at Matruh sub-basin north Western Desert-Egypt," *Delta Journal of Science*, vol. 18, no. 2, pp. 149–159, 1994.

[4] A. N. Shahin, "Undiscovered petroleum reserves in Northern Western Desert, Egypt," in *Proceedings of the 1st International Conference Geology of the Arab World*, pp. 30-31, Cairo, Egypt, 1992.

[5] N. Sultan and A. Halim, "Tectonic Framework of northern Western Desert, Egypt and its effect on hydrocarbon accumulations," in *Proceedings of the EGPC Ninth Exploration Conference*, Cairo, Egypt, 1988.

[6] Mid-oil Company, "Stratigraphic column, Matruh area, Western Desert," Internal report, 1983, Mid-oil Company, 1983.

[7] F. I. Metwalli and J. D. Pigott, "Analysis of petroleum system criticals of the Matruh-Shushan Basin, Western Desert, Egypt," *Petroleum Geoscience*, vol. 11, no. 2, pp. 157–178, 2005.

[8] M. F. Ghanem, M. M. Hammad, and A. F. Maky, "Organo-geochemical evaluation of the subsurface lower Cretaceous rocks of Matruh Basin, North Western desert, Egypt," *El Minia Science Bulletin*, vol. 10, no. 2, pp. 81–107, 1997.

[9] A. F. Douban, "Basin analysis and hydrocarbon potentiality of Matruh basin, North Western Desert, Egypt," in *Proceedings of the Third International Conference for Geology of the Arab World*, pp. 595–624, Cairo University, Cairo, Egypt, 1996.

[10] G. Hantar, "North Western Desert," in *The Geology of Egypt*, R. Said, Ed., pp. 293–319, Balkema Publishers, Rotterdam, Netherlands, 1990.

[11] H. Schandelmeier, E. Klitzsch, F. Hendriks, and P. Wycisk, "Structural development of North-East Africa since Precambrian times," in *Berliner Geowissenschaftliche Abhandlungen*, vol. 75 of *Reihe A: Geologie und Palaeontologie*, pp. 5–24, 1987.

[12] R. Guiraud, "Mesozoic rifting and basin inversion along the northern African Tethyan margin: an overview," *Geological Society, London, Special Publications*, vol. 132, pp. 217–229, 1998.

[13] I. M. Hussein and A. M. A. Abd-Allah, "Tectonic evolution of the northeastern part of the African continental margin, Egypt," *Journal of African Earth Sciences*, vol. 33, no. 1, pp. 49–68, 2001.

[14] W. M. Meshref, "Tectonic framework," in *The Geology of Egypt*, R. Said, Ed., pp. 113–156, Balkema Publishers, Rotterdam, Netherlands, 1990.

[15] W. M. Meshref and H. Hamouda, "Basement tectonic map of northern Egypt," in *Proceedings of the EGPC 9th Exploration and Production Conference*, vol. 1, pp. 55–76, Egyptian General Petroleum Corporation Bulletin, Cairo, Egypt, 1990.

[16] G. Sestini, "Egypt," in *Regional Petroleum Geology of the World. 22*, H. Kulke, Ed., vol. 3, pp. 23–46, Gebruder Borntraeger, Berlin, Germany, 1994.

[17] M. M. Ali, *Geophysical study on Matruh area, Northern part of the Western Desert of Egypt [M.S. thesis]*, Assiut University, Assiut, Egypt, 1988.

[18] S. F. Said, *Geology, Petrology And Reservoir Development Studies of Umbarka area, Western Desert, Egypt [M.S. thesis]*, Helwan University, Helwan, Egypt, 2003.

[19] J. W. Cowie and M. G. Bassett, "Global stratigraphic chart with geochronometric and magnetostratigraphic calibration," *International Union of Geological Sciences*, vol. 12, no. 2, 1989.

[20] B. P. Tissot, R. Pelet, and P. H. Ungerer, "Thermal history of sedimentary basins, maturation indices, and kinetics of oil and gas generation," *The American Association of Petroleum Geologists Bulletin*, vol. 71, no. 12, pp. 1445–1466, 1987.

[21] C. Barker, *Thermal Modeling of Petroleum Generation: Theory and Application*, vol. 45, Elsevier, New York, NY, USA, 1996.

[22] J. D. Pigott and M. O. Abouelresh, "Basin deconstruction-construction: Seeking thermal-tectonic consistency through the integration of geochemical thermal indicators and seismic fault mechanical stratigraphy - Example from Faras Field, North Western Desert, Egypt," *Journal of African Earth Sciences*, vol. 114, pp. 110–124, 2016.

[23] P. A. Allen and J. R. Allen, *Basin Analysis: Principles And Applications*, Blackwell Scientific Publications, Oxford, UK, 1990.

[24] M. L. Keeley and M. S. Massoud, "Tectonic controls on the petroleum geology of NE Africa," *Geological Society, London, Special Publications*, vol. 132, pp. 265–281, 1998.

[25] N. V. Lopatin, "Temperature and geologic time as factors in coalification," *Izvestia Akademii Nauk USSR, Seriya Geologicheskaya*, vol. 3, pp. 95–106, 1971.

[26] D. W. Waples, "Time and temperature in petroleum formation: application of Lopatin's method to petroleum exploration," *The American Association of Petroleum Geologists Bulletin*, vol. 64, no. 6, pp. 916–926, 1980.

[27] D. McKenzie, "Some remarks on the development of sedimentary basins," *Earth and Planetary Science Letters*, vol. 40, no. 1, pp. 25–32, 1978.